Pulsating Flow in a Planar Diffuser Upstream of Automotive Catalyst Monoliths: A CFD Study

Sophie J. Porter[1], Jonathan M. Saul[1], Ahmad K. Mat Yamin[2], Svetlana Aleksandrova[1], Stephen F. Benjamin[1,*], Humberto J. Medina[1]

[1]Faculty of Engineering & Computing, Coventry University, Coventry, UK
[2]Faculty of Mechanical Engineering, Universiti Teknikal Malaysia Melaka, Malaysia
[*]corresponding author: s.benjamin@coventry.ac.uk

Abstract Catalytic converters are used in the automotive industry to reduce pollutant emissions, however maldistribution of flow in the catalyst strongly affects its conversion efficiency. Computational fluid dynamics (CFD) is commonly employed to model flow behaviour. This study investigates the application of CFD to a two-dimensional system consisting of a catalyst monolith downstream of a wide-angled planar diffuser presented with pulsating flow. Flow predictions are compared to particle image velocimetry (PIV) flow fields in the diffuser. A porous medium approach is used for modelling the flow inside the catalyst monolith, with an entrance effect accounting for extra pressure losses due to oblique entry. Predicted velocities show good qualitative agreement with experimental data, with CFD predicting less mixing in the shear layer between the central jet and the recirculation regions. This can be explained by the inability of the turbulence model (unsteady Reynolds Stress Transport) to accurately predict turbulent diffusion. Vorticity in the diffuser is in good qualitative agreement, however CFD predicts higher magnitudes than PIV and the model shows considerably higher residual vorticity at the end of the cycle. As well as the low turbulence diffusion in the model, dissimilarity of vorticity fields is also potentially attributed to cyclic variability in the measured flow field.
Keywords: catalyst, planar diffuser, pulsating flow, CFD, PIV

Notation			
ΔP_{obl}	oblique entry pressure losses, Pa	T	pulse period, s
ΔP_{uni}	unidirectional flow pressure losses, Pa	t	time, s
ρ	density, kg/m^{3}s	U	cycle-averaged mean inlet velocity, m/s
ω	vorticity magnitude, Hz	u	axial velocity, m/s
J	=UT/L	u_s	superficial velocity, m/s
L	length of diffuser, m	v	tangential velocity, m/s

1 Introduction

Catalytic converters are used in the automotive industry to comply with increasingly stringent emissions regulations. The catalyst is generally a monolith consisting of several thousand channels of small hydraulic diameter. Precious metals are embedded in a washcoat applied to the channel walls. Fluid flow behaviour in the system affects the efficiency and durability of the catalytic converter. Air in the exhaust system is turbulent and strongly pulsating. Space constraints necessitate the use of wide-angled diffusers to connect the exhaust pipe to the catalyst. This abrupt expansion causes separation of the flow at the diffuser inlet so that recirculation regions form in the diffuser. Flow in the channels is usually laminar and boundary layers develop at the channel walls as the flow progresses through the monolith.

Measuring the flow in a catalyst system is challenging. Computational fluid dynamics (CFD) provides an alternative approach for determining flow behaviour and is increasingly employed to assess the merits of different designs. It is therefore essential that a model is reliable and predicts flow behaviour with sufficient accuracy. The model is required to accurately simulate flow behaviour in the diffuser and also predict pressure losses associated with the monolith. Solving the entire flow field has been shown to yield CFD predictions with consistent accuracy [1], however resolving the flow in individual channels incurs high computational demand. The common method of modelling the monolith as a porous medium with a prescribed resistance provides a computationally inexpensive approach to representing the intricate geometry of the substrate.

Losses associated with unidirectional flow in the channels may be derived via theoretical calculations or experimental measurements. Benjamin et al. [2] observed an underestimation of flow maldistribution by CFD using this approach,

owing to the simplicity of the model for pressure loss in the monolith. Immediately upstream of the monolith the flow spreads radially, resulting in oblique angles of flow at the monolith face. A recirculation bubble is then formed at the wall of each monolith cell as the highly tangential flow enters the channels, as demonstrated in Figure 1. Quadri et al. [3] and Persoons et al. [4] measured the effect of oblique entry, concluding that pressure losses at locations of oblique flow into the monolith were non-negligible. An expression for these losses, given in Eq. 1, was derived by Küchemann and Weber during their work on heat exchangers [5].

$$\Delta P_{obl} = \frac{\rho v^2}{2} \tag{1}$$

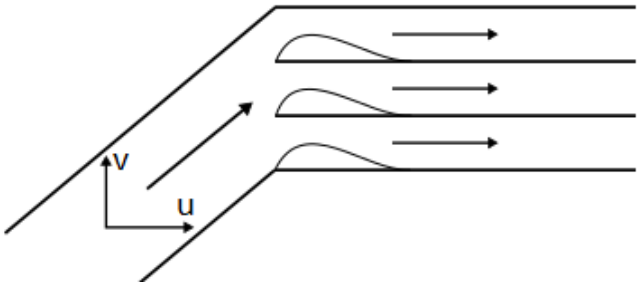

Fig. 1 Schematic diagram of recirculation bubbles formed at channel walls due to oblique flow

A previous study by the authors [1] investigated the application of CFD to steady flow in a planar catalyst system. Flow predictions were compared with particle image velocimetry (PIV) flow fields in the diffuser and hot-wire anemometry (HWA) profiles downstream of the monolith. Two methods of modelling the monolith were studied: porous medium and individual channels. Results showed that the approach used to model the monolith had negligible impact upon predicted flow fields within the diffuser, since the two methods adequately described the high resistance met at the monolith face. Downstream of the monolith predictions varied markedly, demonstrating the importance of the modelling approach when resolving flow entering and exiting the monolith substrate. In the diffuser, the CFD models were found to underestimate the level of mixing in the shear layer located on the jet periphery.

Arias-García et al. [6] observed that pulsating flow resulted in a reduced flow maldistribution downstream of the monolith when compared to the equivalent steady case. Additionally, comparing pulsating flow at different flow rates, Benjamin et al. [7] saw an increased maldistribution downstream of the monolith for higher flow rates. These correlations between flow uniformity and transience and flow uniformity and mass flow rate were confirmed for flow in the diffuser by Mat Yamin et al. [8]. Liu et al. [9] and Benjamin et al. [7] performed transient CFD simulations for comparison with experimental data, finding improved agreement when an entrance effect was incorporated into the model. Velocities were best matched in the central region, with discrepancies regarding flow maldistribution near the wall.

2 Methodology

This paper presents the study of a pulsating flow with frequency 50 Hz and Reynolds number 2.2×10^4, defined by the cycle-averaged mean inlet velocity and the hydraulic diameter of the nozzle. The pulse shape is shown in Figure 2. The flow may be characterised by the non-dimensional parameter $J = 3.6$ derived by Benjamin et al. [10]. J represents the ratio of pulse time (T) to residence time within the diffuser. Mat Yamin et al. [8] found that two flows with a common J factor resulted in similar flow fields within the diffuser.

2.1 Experimental Data Collection

Figure 3 shows a schematic diagram of the isothermal flow rig used by Mat Yamin et al. [8] for measurements of pulsating flow. Air is supplied through a viscous flow meter (1) and enters a plenum (2) with flow straightener (3) and axisymmetric nozzle (4). The air passes through a pulse generator (5) [7] and flow straightener. A resonator box (7) helps shape pulses. A second plenum (8) is supplied with seeding by a particle generator (9). A flow straightener (10) minimises swirling of the flow before it passes through a planar nozzle (11), resulting in approximately uniform flow upon inlet to the planar diffuser (12). The diffuser is made of crown glass, providing optimal visibility for PIV. It has inlet dimensions 24 × 96 mm, outlet dimensions 78 × 96 mm, length 48 mm and total included angle of approximately 60°. The diffuser outlet is attached to a 27 mm long unwashed cordierite monolith (13) with channel hydraulic diameter 1.12

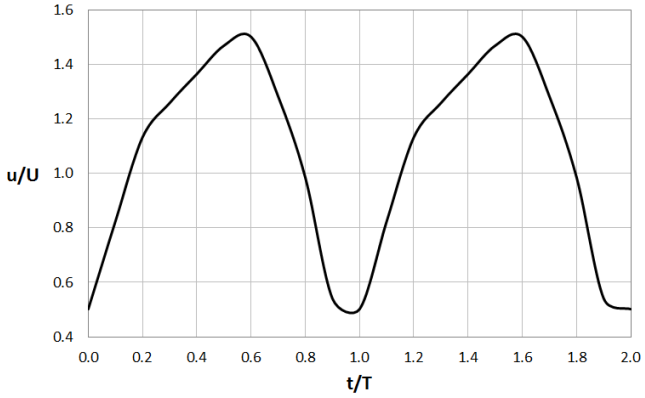

Fig. 2 Cycle-averaged inlet velocity at centre of nozzle

mm, nominal cell density 62 cells per cm^2 and porosity 0.77. An outlet sleeve (14) of length 50 mm and dimensions 125 × 137 mm minimised any influence from air outside of the rig. Flow within the diffuser was measured using PIV. Seeding

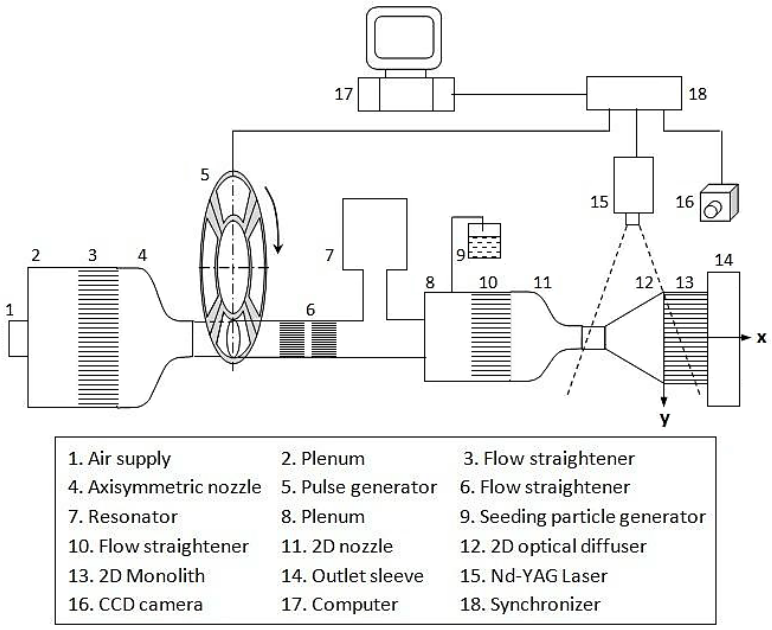

Fig. 3 Schematic diagram of 2D isothermal flow rig

was provided using a six-jet atomiser at 25 psi with olive oil, producing droplets of approximately 0.6 μm diameter. A cylindrical lens of -25 mm focal length was combined with a 500 mm spherical lens. A 120 mJ solid-state Nd:YAG laser was thereby transformed into a 0.5 m stand-off light sheet approximately 1 mm thick to illuminate the seeded flow. A 4-megapixel CCD camera with 2048 × 2048 pixel (1 pixel = 7.4 μm) resolution captured the flow field. The camera was coupled with a 105 mm lens and placed 0.8 m from the measurement plane, resulting in an 80 × 60 mm field of view with a magnification factor of 0.155. A focal ratio of 11 ensured a particle image diameter greater than 2 pixels, avoiding pixel locking. Image processing was effected using INSIGHT-3G software. The recursive Nyquist method with 64 × 64 initial grid and 32 × 32 final grid yielded 95% valid vectors in each field and a vector resolution of 0.76 mm.
The majority of the flow field in the diffuser was captured. The sealed joint at the inlet to the diffuser impeded visibility and so some data loss is present. It was also not possible to obtain measurements close to the monolith face (< 2.5 mm).

2.2 Computational Method

Simulations were performed using the commercial CFD solver STAR-CCM+. The time-dependent isothermal air flow in the system was found to be symmetric and two-dimensional [8]. It is therefore sufficient for computational purposes to resolve a two-dimensional domain with half-widths of the diffuser, monolith and outlet sleeve. The model geometry is shown in Figure 4. The high resistance of the monolith is treated by modelling the region as a porous medium with a

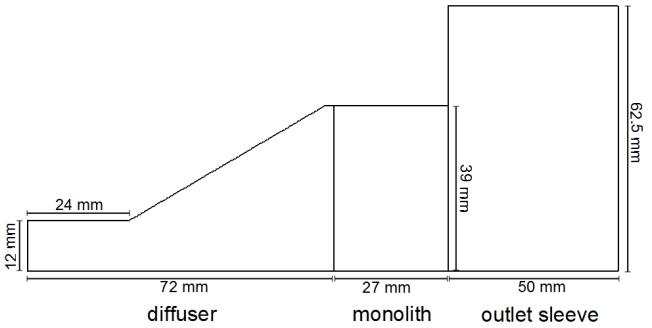

Fig. 4 Two-dimensional computational flow domain

prescribed axial pressure loss derived from experimental measurements. The pressure drop associated with unidirectional flow along the monolith length is expressed as a second-order polynomial function of the superficial velocity of the system, as given in Eq. 2. ΔP_{uni} denotes the pressure loss per unit length and the second- and first-order term coefficients are the scalar coefficients of the inertial (kg/m^4) and viscous (kg/m^3s) resistance tensors respectively. Tangential resistance tensors of 10^7 ensure unidirectional flow. The additional pressure loss term given by Eq. 1 accounts for pressure losses associated with oblique entrance angle.

$$\Delta P_{uni} = 14.1\, u_s{}^2 + 734\, u_s \tag{2}$$

Turbulence is modelled using the linear pressure-strain two-layer Reynolds Stress Transport model. The linear pressure-strain model of Gibson and Launder [11] is incorporated into a two-layer (shear driven) formulation as suggested by Rodi [12]. Since transport equations are solved for all specific Reynolds stress tensor components, the model inherently accounts for anisotropy of the turbulent stress field [13]. A second-order upwind convection scheme is used. At the inlet, the turbulence intensity (0.01) and viscosity ratio (10) are constant and uniform. Velocity is uniform and periodic, as per experimental measurements. Inlet velocities were extracted directly from PIV data and interpolated using spline interpolation. The geometry was meshed on a regular hexahedral grid with prism layers at the walls to capture the developing boundary layer. Time-dependent simulations were initiated from a fully-converged equivalent steady solution and flow predictions were extracted after 10 cycles, by which point the solution had reached sufficient periodicity.

3 Results and Analysis

Flow fields in the diffuser from PIV and CFD are compared at regular non-dimensional times throughout the pulse cycle. PIV data is averaged from 100 individual cycles. Figure 5 shows velocity vector fields. Velocities are normalised by the cycle-averaged mean inlet velocity. Figure 6 shows vorticity contours in the diffuser. The non-dimensional unit ωL/U denotes the normalisation of the vorticity magnitude by the diffuser length and the cycle-averaged mean inlet velocity.

Peak inlet velocity occurs at t/T = 0.6. High inertia at the diffuser inlet causes separation of the flow from the wall, resulting in a jet which traverses the diffuser. The jet spreads immediately upstream of the monolith face. Flow either enters the monolith or forms large recirculating regions either side of the jet. The shear layer at the jet edge is then incorporated into the recirculation region. At time t/T = 0.8 the flow field is similar to the steady state case [1][8]. During inlet flow deceleration (t/T = 0.7–1.0) the recirculation regions dominate the diffuser and the central jet width is narrowed as a result of pulsation [14]. Vorticity decreases and dissipates within the diffuser. Acceleration of the inlet flow (t/T = 0.1–0.5) sees the residual vortices of the previous cycle carried along the length of the diffuser, with flow reattaching. Increasing inertia then causes the flow to detach again, at around t/T = 0.4. Flow is able to reattach to the diffuser wall downstream of the small recirculation bubble, resulting in a relatively uniform velocity profile upon exit from the diffuser.

Comparing experimental results with the numerical model, best qualitative agreement is observed mid-cycle, for t/T = 0.4–0.8. PIV shows high variation of the jet core width, noticeably smaller at t/T = 0.1 than during the rest of the cycle. For high inlet velocities, PIV data see more diffusion of the jet, with the shear layer wider than for CFD. There is significant difference in vortex structure at timesteps t/T = 0.1–0.3, where residual vorticity is negligible for PIV data. The retention of vorticity by CFD suggests an underestimation of turbulent dissipation.

In Figure 6, CFD shows high vorticity magnitudes at vortex centres and within the jet shear layer. Maximum PIV vorticity magnitudes are low in comparison throughout the cycle. For example, at t/T = 0.7 the predicted vorticity at the centre of the vortex is twice as high as PIV measurements. The disagreement between CFD and PIV may be explained by one or

more of the following. Firstly, it is possible that the computational model does not accurately predict the turbulent characteristics of the flow. Turbulence modelling is a complex field with many variables and no one model to suit all flows. Another reason for the difference in values is the level of data resolution. The computational model is more refined than the PIV data set. It is possible that the interrogation window used for PIV measurements was too large to capture high velocity gradients. Finally, it must be noted that the post-processed PIV data have been phase-averaged from multiple cycles. Any cyclic variation in vortex location would then result in the absence of higher vorticity magnitudes once all cycles are averaged.
Difference in vortex strength between PIV and CFD is attributable to variation in location from cycle to cycle, not accounted for in the numerical model. The variation between the instantaneous flow field and the corresponding phase-average is the subject of ongoing research by the authors [15].

4 Conclusion

CFD simulations have been performed for pulsating flow in a two-dimensional catalytic converter system with a wide-angled planar diffuser. Predictions from the model are compared with experimental measurements taken by PIV in the diffuser. Velocity fields in the diffuser are in good qualitative agreement with PIV data. Vortex structures in the diffuser are well-matched mid-cycle, however maximum vorticity levels at the centre of the large vortex structures are approximately twice as high for CFD than as presented by the phase-averaged PIV data. Post-separation, large recirculation regions present in CFD show higher residual vorticity. As well as the low turbulence diffusion of the model, dissimilarity in vortex strength between PIV and CFD may also be attributable to cyclic variation.

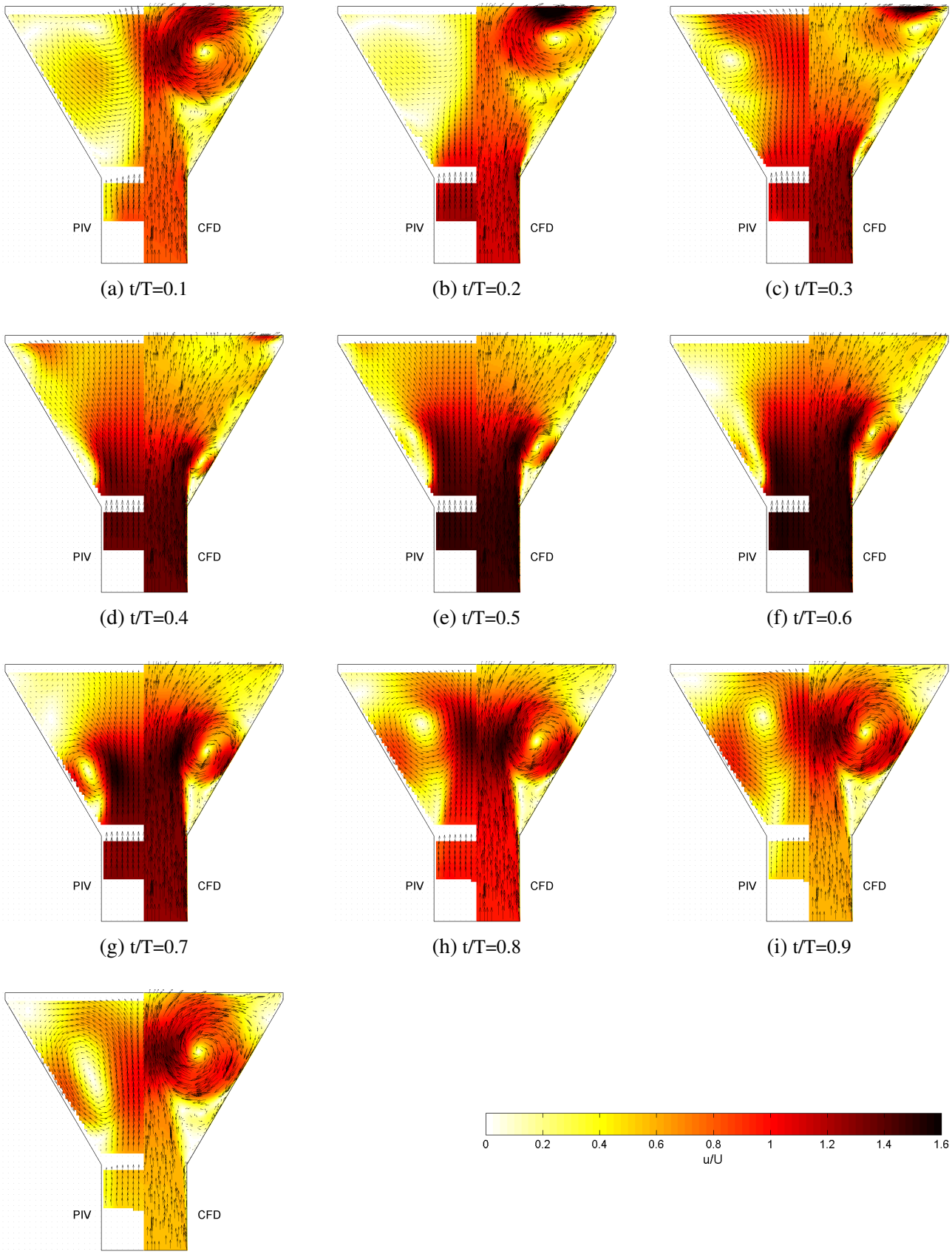

(a) t/T=0.1 (b) t/T=0.2 (c) t/T=0.3

(d) t/T=0.4 (e) t/T=0.5 (f) t/T=0.6

(g) t/T=0.7 (h) t/T=0.8 (i) t/T=0.9

(j) t/T=1.0

Fig. 5 Velocity vector fields normalised by the cycle-averaged mean inlet velocity.

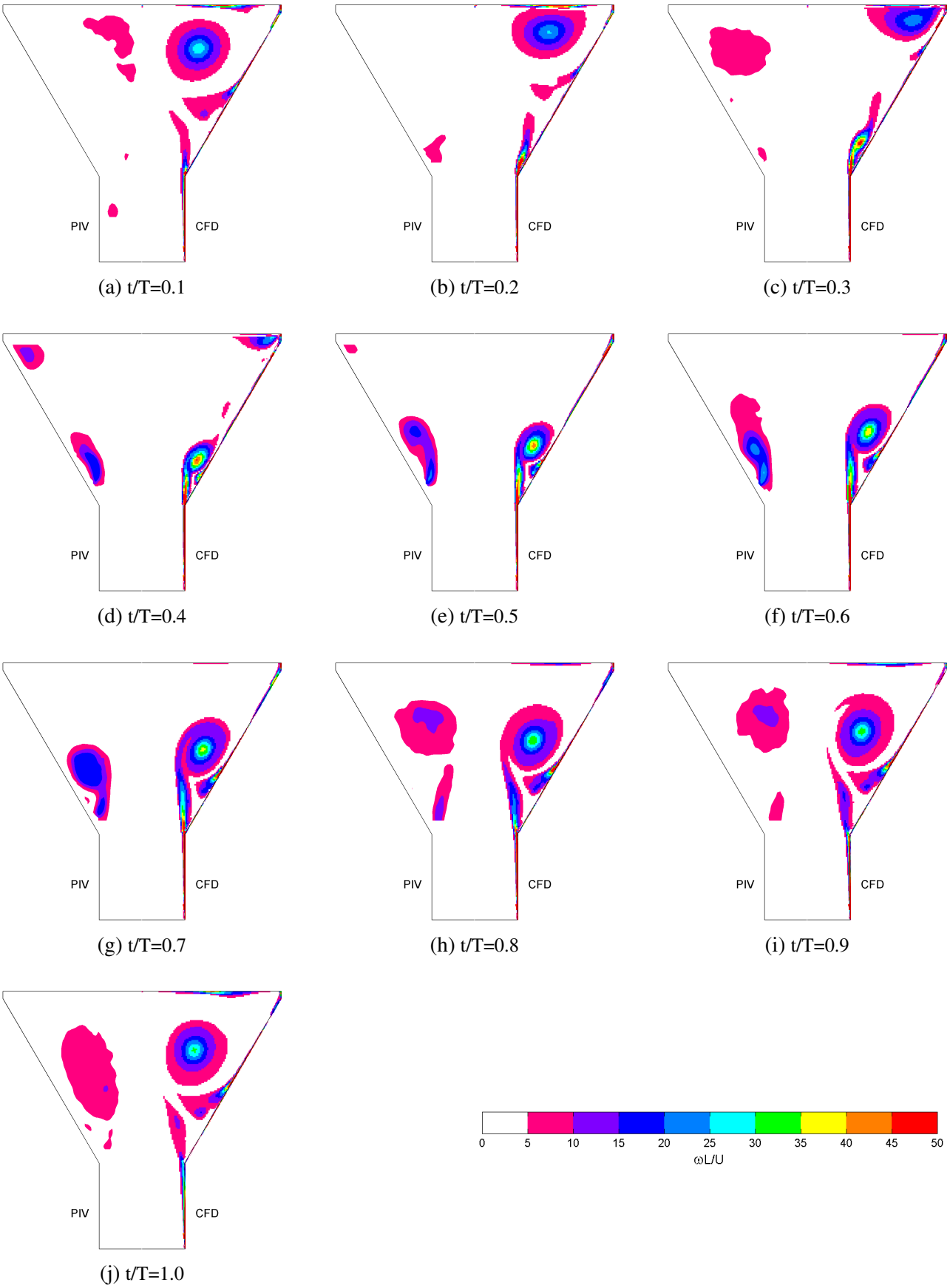

(a) t/T=0.1 (b) t/T=0.2 (c) t/T=0.3

(d) t/T=0.4 (e) t/T=0.5 (f) t/T=0.6

(g) t/T=0.7 (h) t/T=0.8 (i) t/T=0.9

(j) t/T=1.0

Fig. 6 Vorticity contours normalised by the length of the diffuser and the cycle-averaged mean inlet velocity.

References

[1] Porter S J, Mat Yamin A K, Aleksandrova S, Benjamin S F, Roberts C A, Saul J M (2014) An assessment of CFD applied to steady flow in a planar diffuser upstream of an automotive catalyst monolith. *SAE International Journal of Engines*, vol. 7, pp 1697-1704. doi: 10.4271/2014-01-2588.

[2] Benjamin S F, Clarkson R J, Haimad N, Girgis N S (1996) An experimental and predictive study of the flow field in axisymmetric automotive exhaust catalyst systems. SAE Technical Paper 961208. doi: 10.4271/961208

[3] Quadri S S, Benjamin S F, Roberts C A (2009) An experimental investigation of oblique entry pressure losses in automotive catalytic converters. In: Proceedings of the Institution of Mechanical Engineers, Part C: Journal of Mechanical Engineering Science, vol. 223, pp 2561-2569. doi: 10.1243/09544062JMES1565

[4] Persoons T, Vanierschot M, Van den Bulck E (2008) Oblique inlet pressure loss for swirling flow entering a catalyst substrate. *Experimental Thermal and Fluid Science*, vol. 32 (6), pp 1222-1231. doi: 10.1016/j.expthermflusci.2008.02.002

[5] Küchemann D, Weber J (1953) Aerodynamics of propulsion. McGraw-Hill, New York

[6] Arias-García A, Benjamin S F, Zhao H, Farr S (2001) A comparison of steady, pulsating flow measurements and CFD simulations in close-coupled catalysts. SAE Technical Paper 2001-01-3662. doi: 10.4271/2001-01-3662.

[7] Benjamin S F, Roberts C A, Wollin J (2001) A study of the effect of flow pulsations on the flow distribution within ceramic contoured catalysts substrates. *SAE International Journal of Fuels and Lubricants*, vol. 4 (110), pp 1380-1387.

[8] Mat Yamin A K, Benjamin S F, Roberts C A (2013) Pulsating flow in a planar diffuser upstream of automotive catalyst monoliths. *International Journal of Heat and Fluid Flow*, vol. 40, pp 43-53. doi:10.1016/j.ijheatfluidflow.2013.01.014

[9] Liu Z, Benjamin S F, Roberts C A (2003) Pulsating flow maldistribution within an axisymmetric catalytic converter - Flow rig experiment and transient CFD simulation. SAE Technical Paper 2003-01-3070. doi: 10.4271/2003-01-3070

[10] Benjamin S F, Roberts C A, Wollin J (2002) A study of pulsating flow in automotive catalyst systems. *Experiments in Fluids*, vol. 33 (5), pp 629-639. doi: 10.1007/s00348-002-0481-0

[11] Gibson M M, Launder B E (1978) Ground effects on pressure fluctuations in the atmospheric boundary layer. *Journal of Fluid Mechanics*, vol. 86, part 3, pp 491-511.

[12] Rodi W (1991) Experience with two-layer models combining the k-ε model with a one-equation model near the wall. In: Proceedings of the 29th Aerospace Sciences Meeting, AIAA Paper 91-0216.

[13] Hanjalić K, Jakirlić S (2002) Second-moment turbulence closure modelling. In: Launder B E, Sandham N D eds. Closure strategies for turbulent and transitional flows. Cambridge University Press, New York

[14] Medina H J, Benard E, Early J M (2013) Reynolds number effects on fully developed pulsed jets impinging on flat surfaces. *AIAA Journal*, vol. 51 (10), pp 2305-2318. doi: 10.2514/1.J051203

[15] Saul J M, Porter S J, Mat Yamin A K, Medina H J, Aleksandrova S, Benjamin S F (2015) Influence of cyclic variance on the performance of URANS for pulsating flow upstream of an automotive catalyst monolith. Submitted to the IMechE Internal Combustion Engines Conference, London, 2nd-3rd December 2015